Electronic Supporting Information

For

Infinite coordination polymer networks: Metallogelation of aminopyridine conjugates and in situ silver nanoparticle formation

Rajendhraprasad Tatikonda,[a] Evgeny Bulatov,[a] Zülal Özdemir,[d] Nonappa[b,c] and Matti Haukka*[a]*

[a]*Department of Chemistry, University of Jyväskylä, P. O. Box 35, FI-40014 Jyväskylä, Finland.*

[b]*Department of Applied Physics, Aalto University School of Science, Puumiehenkuja 2, FI-02150 Espoo, Finland.*

[c]*Department of Bioproducts and Biosystems, Aalto University School of Chemical Engineering, Kemistintie 1, FI-02150 Espo, Finland.*

[d] *University of Chemistry and Technology in Prague, Faculty of Food and Biochemical Technology,*

Department of Chemistry of Natural Compounds, Technicka 5, 16628 Prague 6, Czech Republic

Experimental section

General considerations

All chemicals were purchased from chemical sources and used without purification. *Caution!!!* No problems were encountered in this work although silver perchlorate is potentially explosive. DMSO and DMF for the gelation test was ACS reagent grade (≥99.9%). NMR spectra (1D and 2D) of ligands and its silver complexes and gels were recorded on a Bruker Avance III HD 300 MHz and 500 MHz NMR spectrometers and chemical shifts are expressed in ppm. Elemental analysis was performed on Vario EL elemental analyser. UV-Vis and photoluminescence spectra was recorded using Perkin Elmer Lambda 650 and Varian Cary Eclipse fluorescence spectrometers respectively.

General synthetic procedure for 4,4'-di (pyridin-3-yl)-[2,2'-bipyridine]-4,4′-dicarboxamide (3) and 4,4'-di (pyridin-4-yl)-[2,2'-bipyridine]-4,4′-dicarboxamide (4)

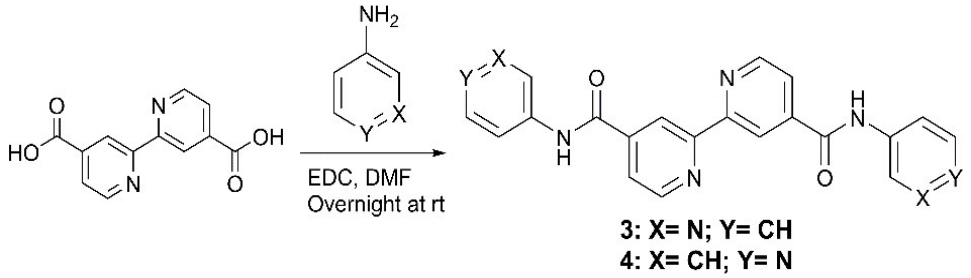

Scheme S1. Synthesis of ligands **3** and **4**.

Procedure: A mixture of 4,4′-dicarboxy-2,2′-bipyridine (0.245 g, 1 mmol), corresponding aromatic amine (0.190 g, 2 mmol) and N-ethyl-N'-(3-dimethylaminopropyl)carbodiimide (0.770 g, 4 mmol) in DMF (5 mL) was stirred at room temperature overnight. After the reaction, the resulting off white solid was filtered and washed with excess of water followed by acetone and dried under vacuum.

Ligand 3: Yield (0.261 g, 71.7%); ^{1}H NMR (300 MHz, DMSO-d_6 at 30 ^{o}C) δ 10.90 (s, 1H), 8.99 (d, 2H), 8.95 (d, 1H), 8.37 (dd, 1H), 8.23 (dq, 1H), 8.01 (dd, 1H), 7.45 (q, 1H). ^{13}C NMR (75 MHz, DMSO-d_6) δ 164.22, 154.86, 150.50, 145.37, 143.07, 142.35, 135.36, 127.94, 123.79, 122.66, 118.99. FTIR: 1678.11 cm-1 (CO), 3233.30 cm-1 (NH). Anal. Calcd for $C_{22}H_{16}N_6O_2$: C, 66.66: H, 4.07; N, 21.20. Found: C, 66.45; H, 4.28; N, 21.00. ESI-TOF-MS Calcd. For $[M+H]^+$ $(C_{22}H_{17}N_6O_2)^+$: 397.1408; found: 397.1425.

^{1}H NMR (500 MHz, DMSO-d_6 at 70^{o}C) δ 10.76 (s, 1H), 8.98 (d, 2H), 8.94 (d, 1H), 8.37 (dd, 1H), 8.22 (dq, 1H), 8.00 (dd, 1H), 7.43 (q, 1H). ^{13}C NMR (125 MHz, DMSO-d_6 at 30^{o}C) δ 164.31, 155.48, 150.26, 145.13, 142.87, 142.21, 135.29, 127.67, 123.60, 122.43, 118.55. ^{1}H-^{15}N COSY NMR (DMSO-d_6 at 70^{o}C) δ -60.00 (Bipy N^B), -62.66 (Py N^P) and -253.37 (Amide N^A).

3●AgNO$_3$: ^{1}H NMR (300 MHz, DMSO-d_6) δ 10.94 (s, 1H), 9.00 (d, 2H), 8.96 (d, 1H), 8.39 (dd, 1H), 8.24 (dq, 1H), 8.05 (dd, 1H), 7.48 (q, 1H). ^{13}C NMR (75 MHz, DMSO-d_6 at 80^{o}C) δ 163.94, 154.95, 149.89, 144.92, 142.79, 142.21, 134.94, 127.62, 123.12, 121.95, 118.56.

^{1}H NMR (500 MHz, DMSO-d_6 at 70^{o}C) δ 10.80 (s, 1H), 8.99 (d, 2H), 8.95 (d, 1H), 8.38 (dd, 1H), 8.22 (dq, 1H), 8.03 (dd, 1H), 7.46 (q, 1H). ^{1}H-^{15}N COSY NMR (DMSO-d_6 at 70^{o}C) δ -64.35 (Bipy N^{B}), -67.23 (Py N^{P}) and -253.16 (Amide N^{A}).

Ligand 4: Yield (0.190 g, 52.2%); ^{1}H NMR (300 MHz, DMSO-d_6) δ 11.03 (s, 1H), 8.99 (d, 1H), 8.91 (d, 1H), 8.53 (dd, 2H), 7.99 (dd, 1H), 7.82 (dd, 2H). FTIR: 1698.68 cm-1 (CO), 3480.43 cm-1 (NH). Anal. Calcd for $C_{22}H_{16}N_6O_2$: C, 66.66: H, 4.07; N, 21.20. Found: C, 66.39; H, 4.20; N, 20.94. ESI-TOF-MS Calcd. For $[M+H]^+$ $(C_{22}H_{17}N_6O_2)^+$: 397.1408; found: 397.1420.

^{1}H NMR (300 MHz, DMSO-d_6 at 80 °C) δ 10.79 (s, 2H), 8.96 (d, 2H), 8.90 (d, 2H), 8.53 (dd, 4H), 7.98 (dd, 2H), 7.80 (dd, 4H). ^{13}C NMR (75 MHz, DMSO-d_6 at 80 °C) δ 164.47, 155.32, 149.90, 149.71, 145.01, 142.47, 121.80, 118.27, 113.99.

4●$AgNO_3$: No solubility was found.

NMR Spectroscopy

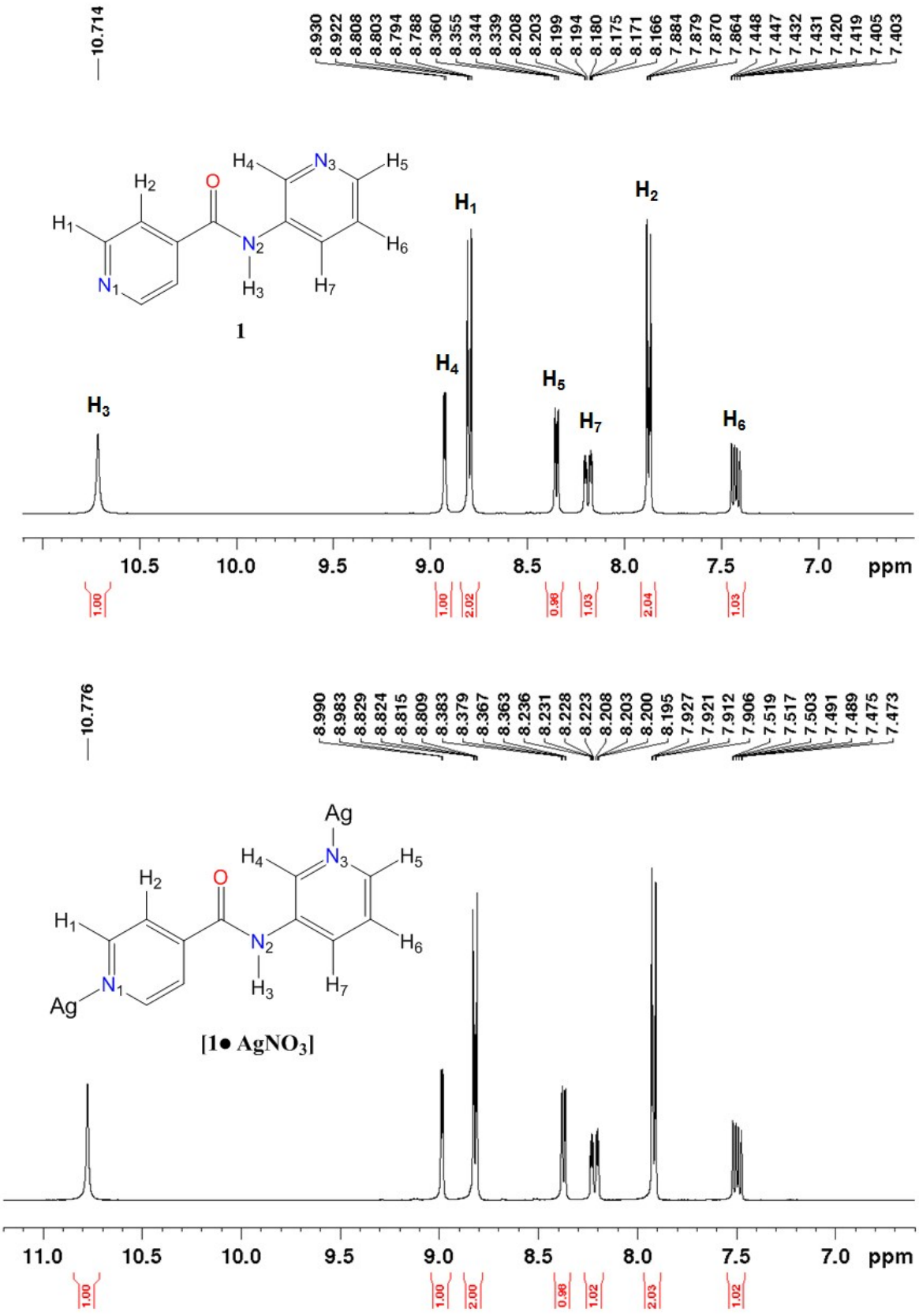

Figure S1. ^{1}H NMR of ligand **1** (top) and **[1_2●$AgNO_3$]** (bottom) in DMSO-d_6 at 30°C.

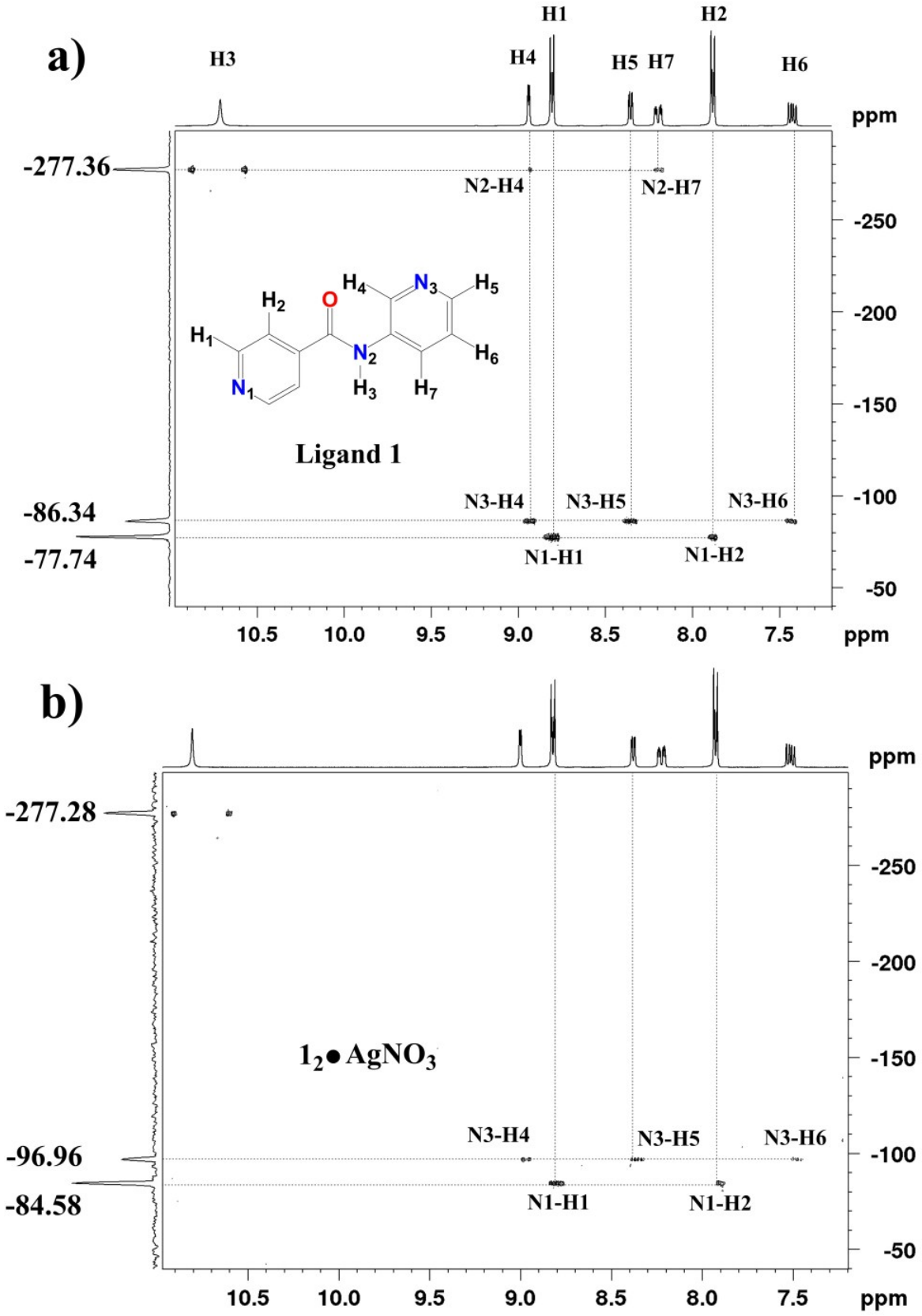

Figure S2. ^{1}H-^{15}N COSY NMR of ligand **1** (a) and its **[1_2●$AgNO_3$]** complex (b) in DMSO-d_6 at 30°C.

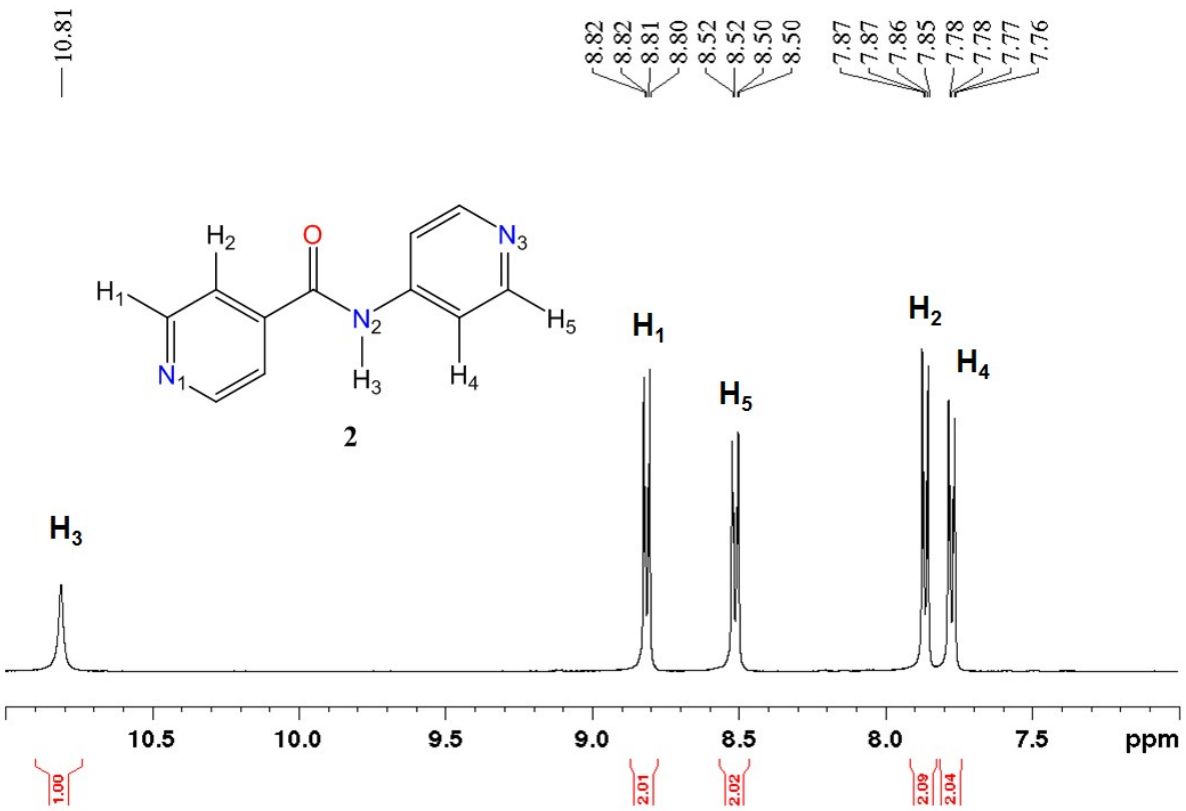

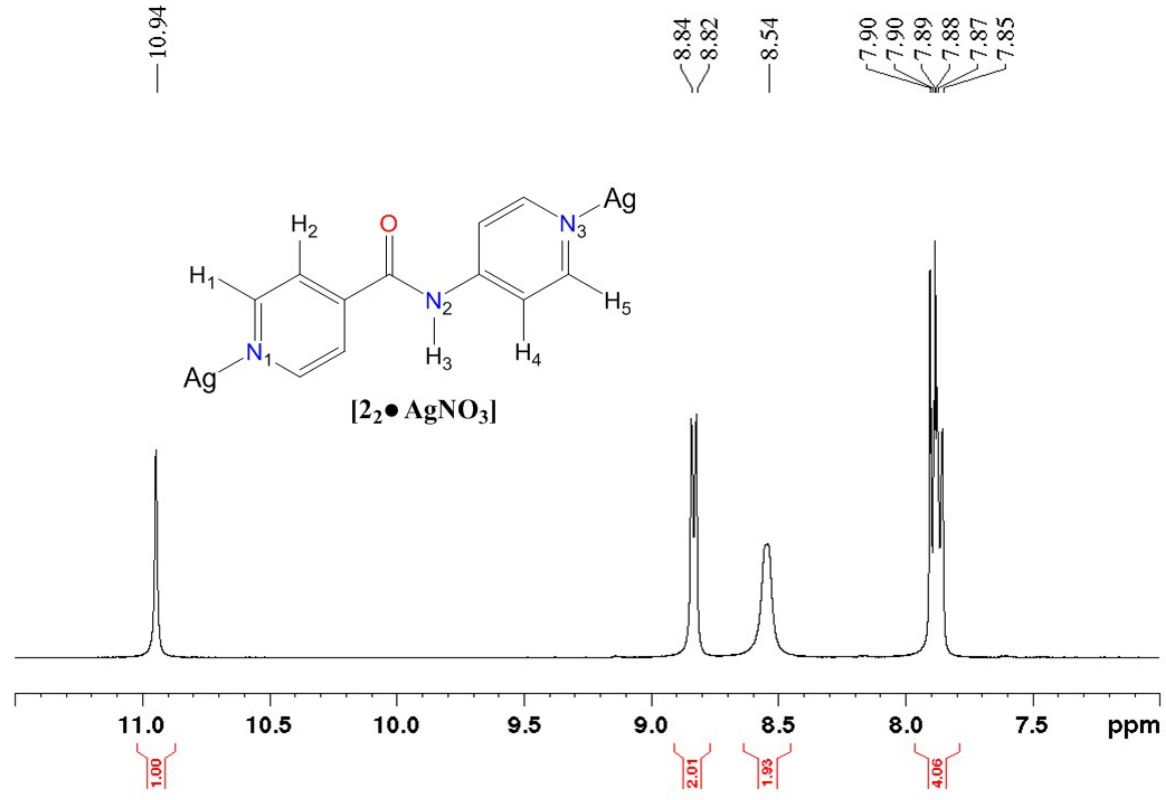

Figure S3. ^{1}H NMR of ligand **2** (top) and **[2_2●$AgNO_3$]** (bottom) in DMSO-d_6 at 30°C

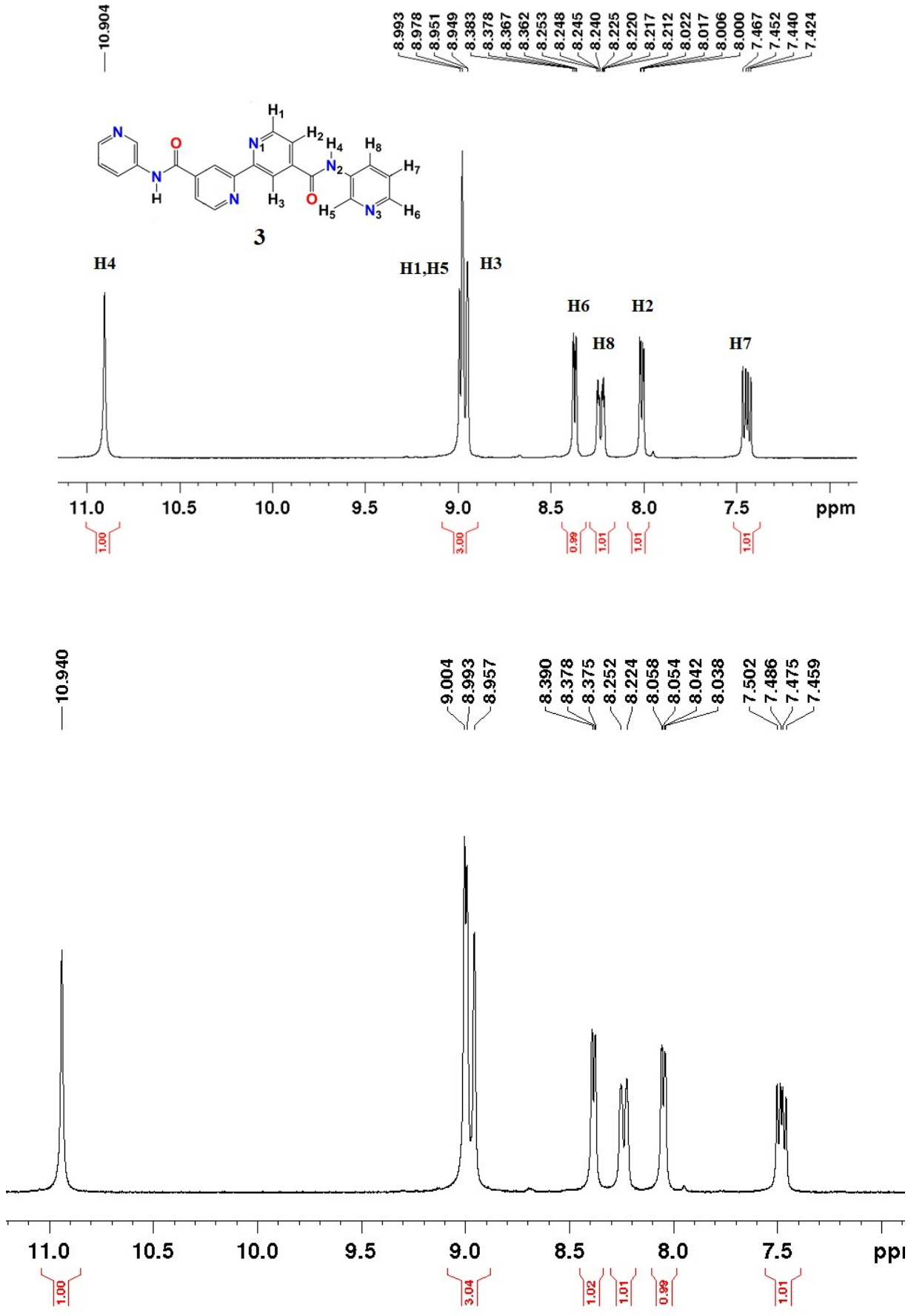

Figure S4. ^{1}H NMR of ligand **3** (top) and **[3●AgNO$_3$]** complex (bottom) in DMSO-d_6 at 30°C.

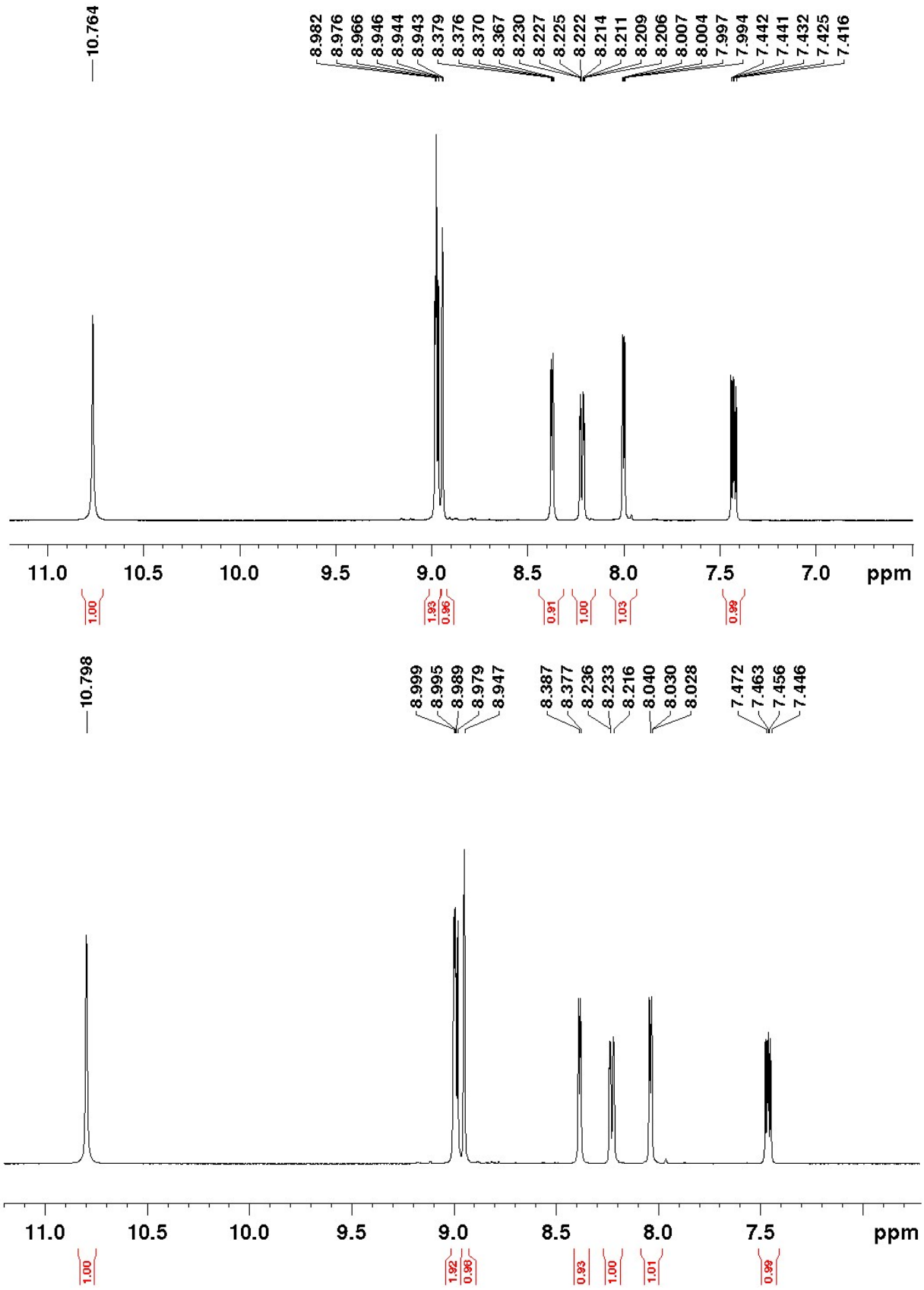

Figure S5. ^{1}H NMR of ligand **3** (top) and **[3●AgNO$_3$]** complex (bottom) in DMSO-d_6 at 70°C.

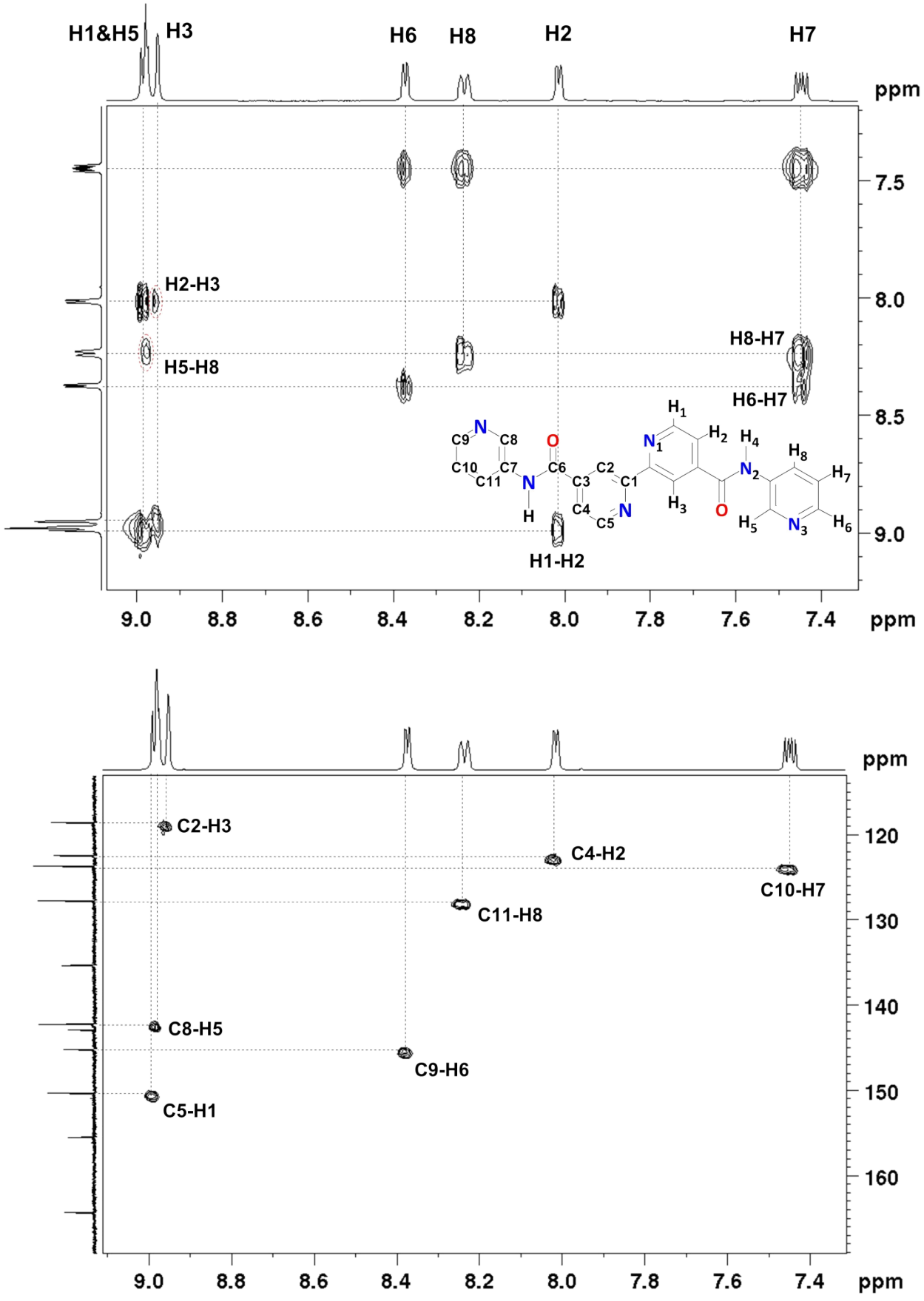

Figure S6. ^{1}H-^{1}H COSY (top) ^{1}H-^{13}C HSQC (bottom) of **3** in DMSO-d_6 at 30°C.

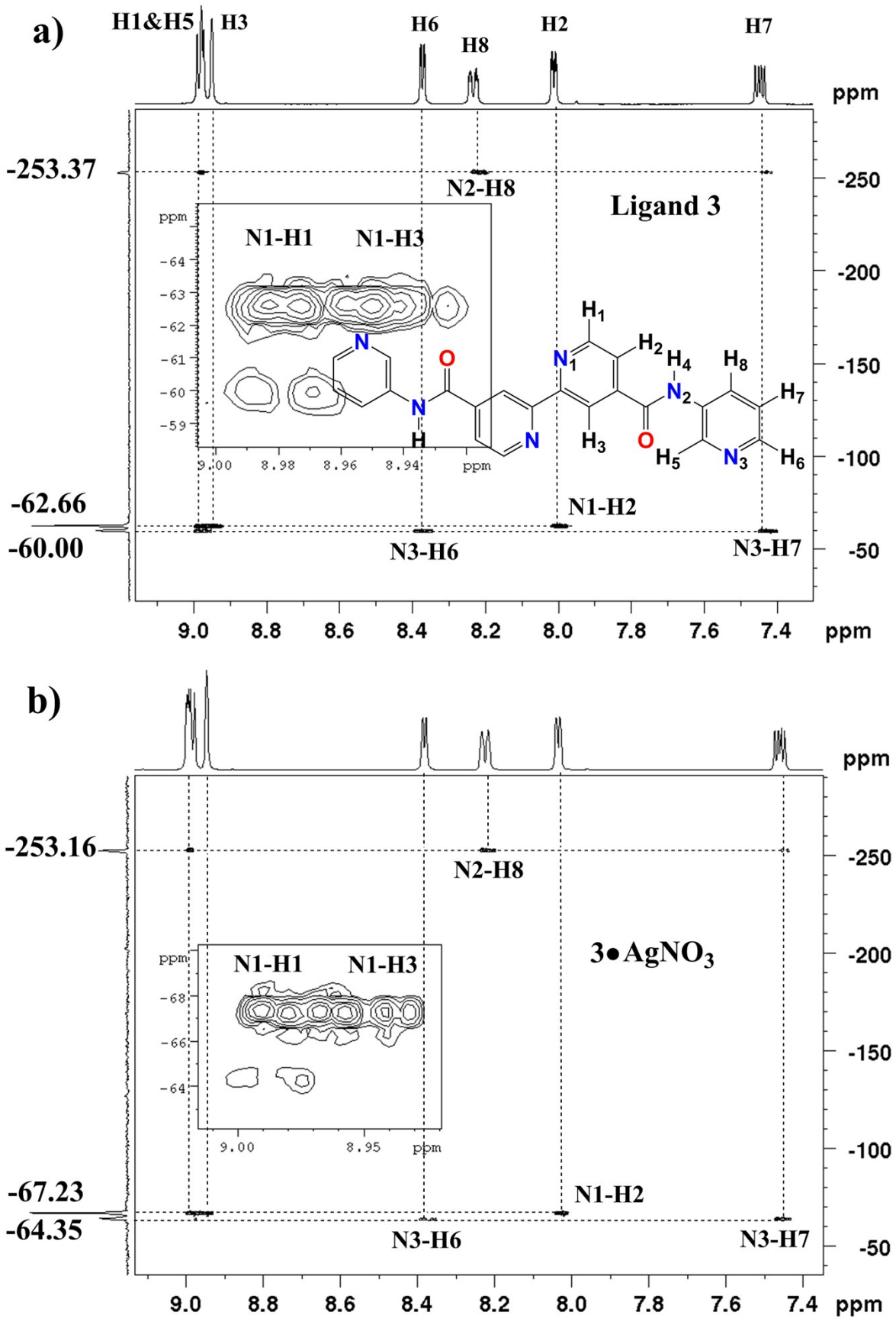

Figure S7. ^{1}H-^{15}N COSY NMR of ligand **3** (a) and its **[3●AgNO$_3$]** complex (b) in DMSO-d_6 at 70°C.

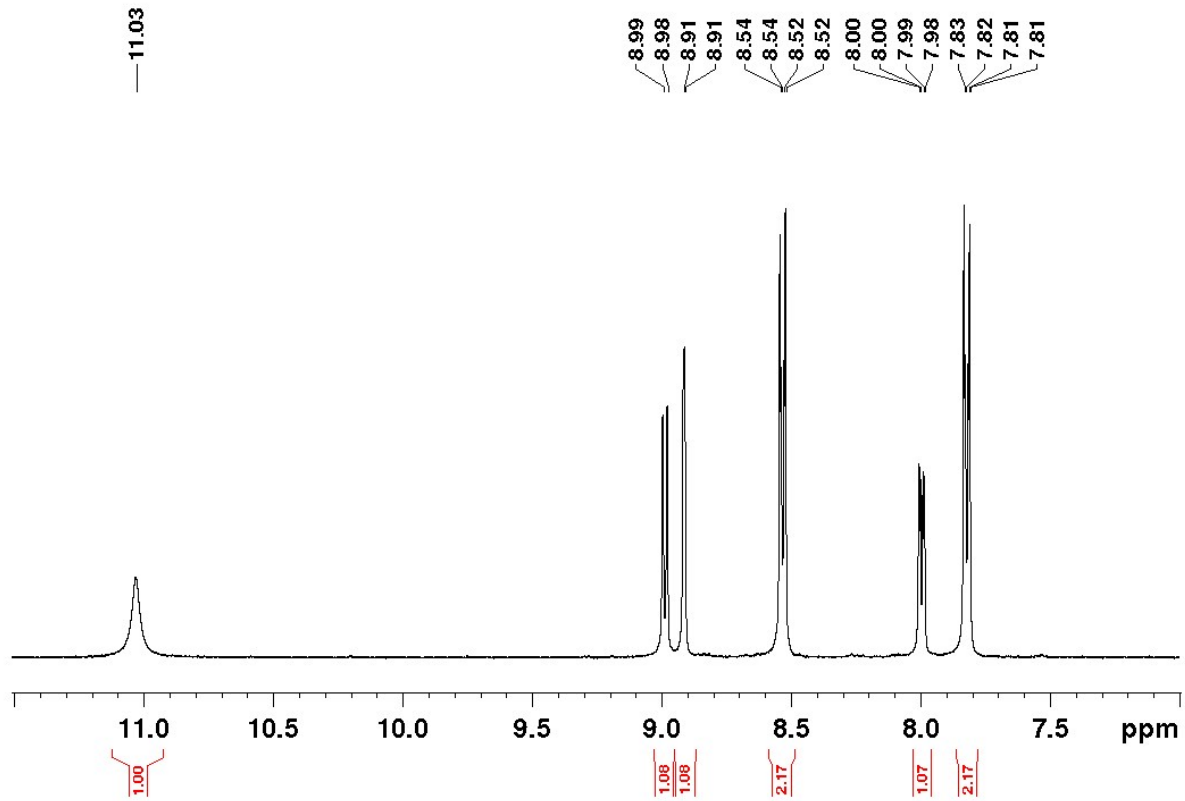

Figure S8. ^{1}H NMR of ligand **4** DMSO-d_6 at 30 °C.

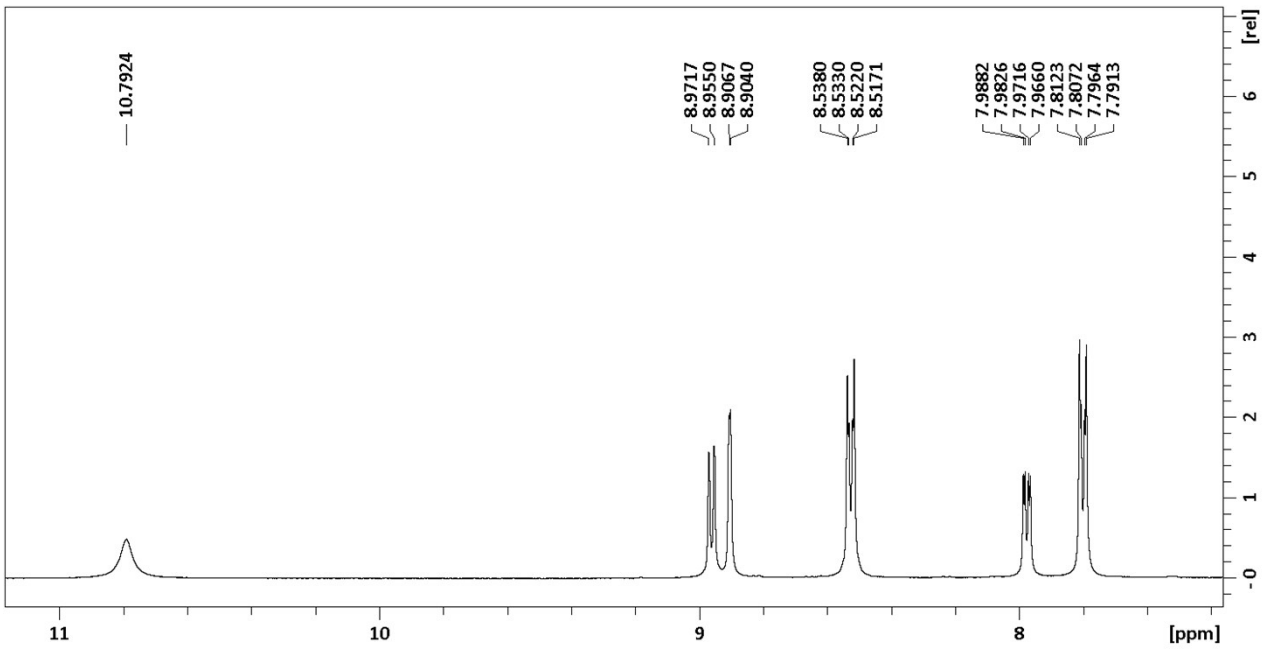

Figure S9. ^{1}H NMR of ligand **4** in DMSO-d_6 at 80 °C.

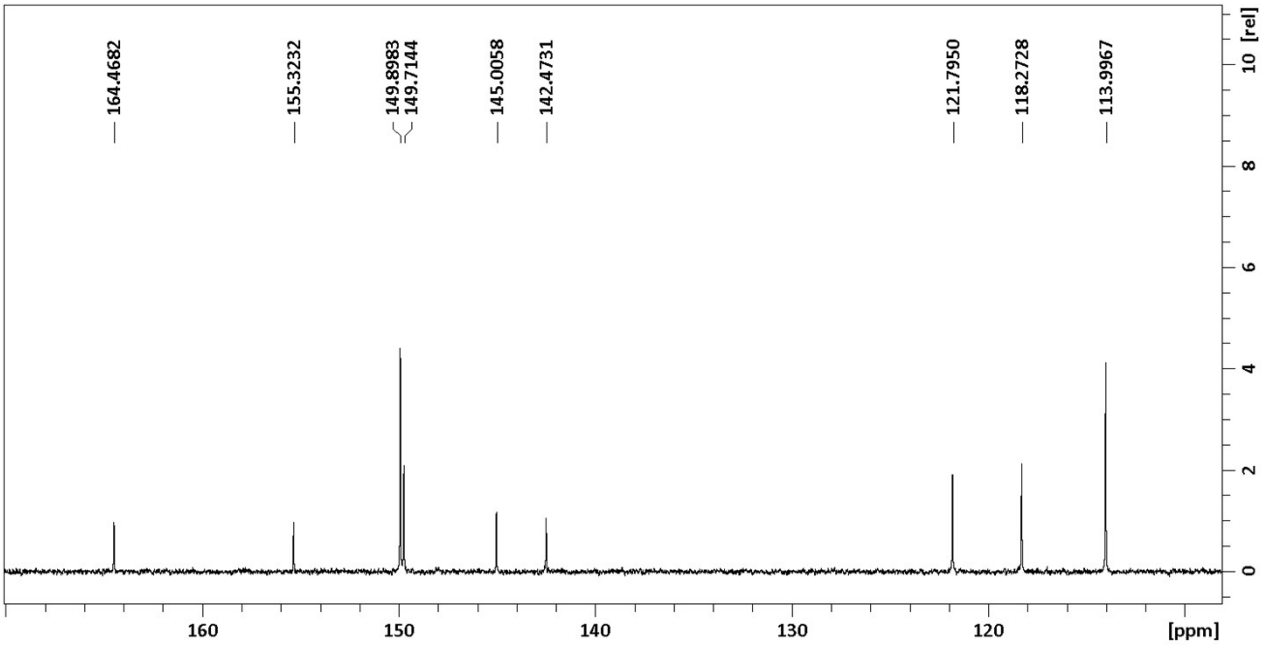

Figure S10. ^{13}C NMR of ligand **4** in DMSO-d_6 at 80°C.

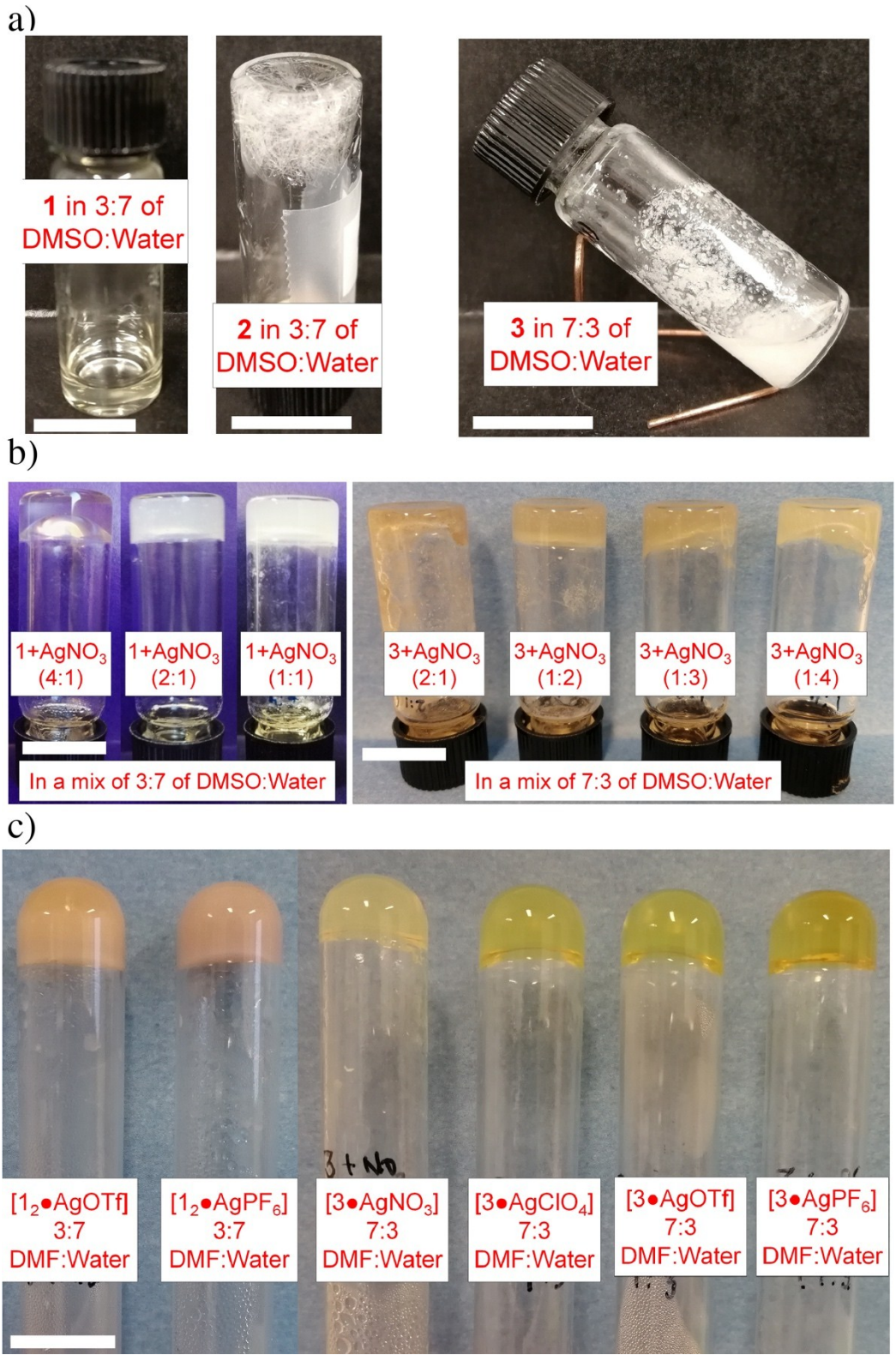

Figure S11. Additional gelation experiments. **a**) ligands **1, 2** and **3** without silver in DMSO: H_2O mixture, **b**) gels prepared from different molar amounts of silver to the ligands **1** and **3** and, **c**) Gels from a mixture of DMF:H_2O. Scale bars: a and b, 15 mm and c, 12 mm.

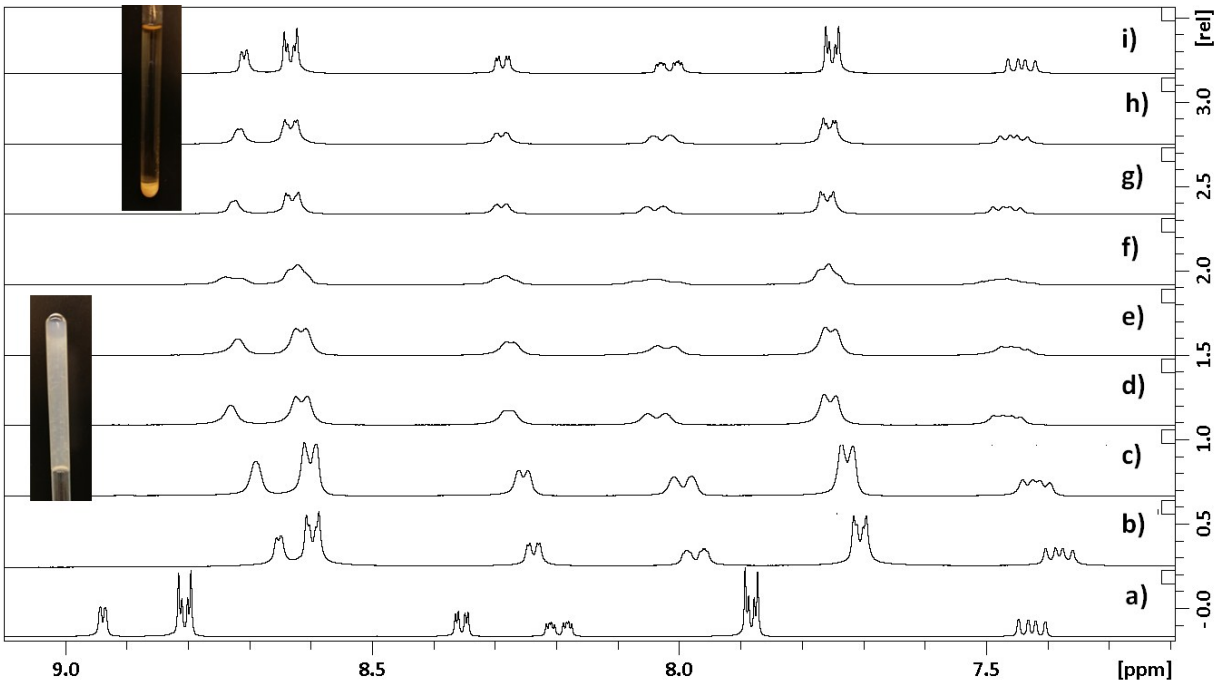

Figure S12. a) Ligand **1** in DMSO, b) **1** in a mixture of DMSO:D_2O (3:7), c) 1+$AgPF_6$ gel (1:1) d-i) 1+$AgPF_6$ gel (2:1) from 30 °C-80 °C with 10 °C increase. (Inlet figures: 1+$AgPF_6$ gel (2:1) before (bottom) and after (top) VT NMR experiment)

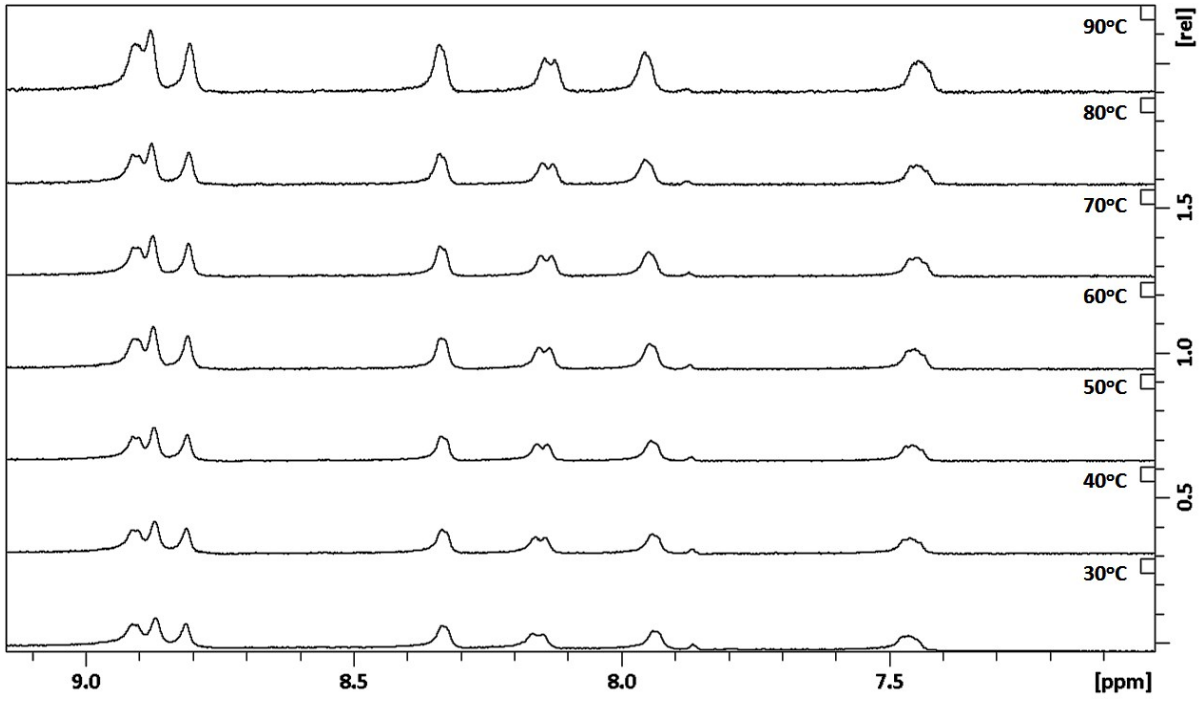

Figure S13. Temperature dependent ^{1}H-NMR spectra of [**3●AgNO$_3$**] gel system (1.6 x 10^{-2} M) from 8:2 of DMSO-d_6:D_2O (from 30 °C to 90 °C, 10 °C step increase).

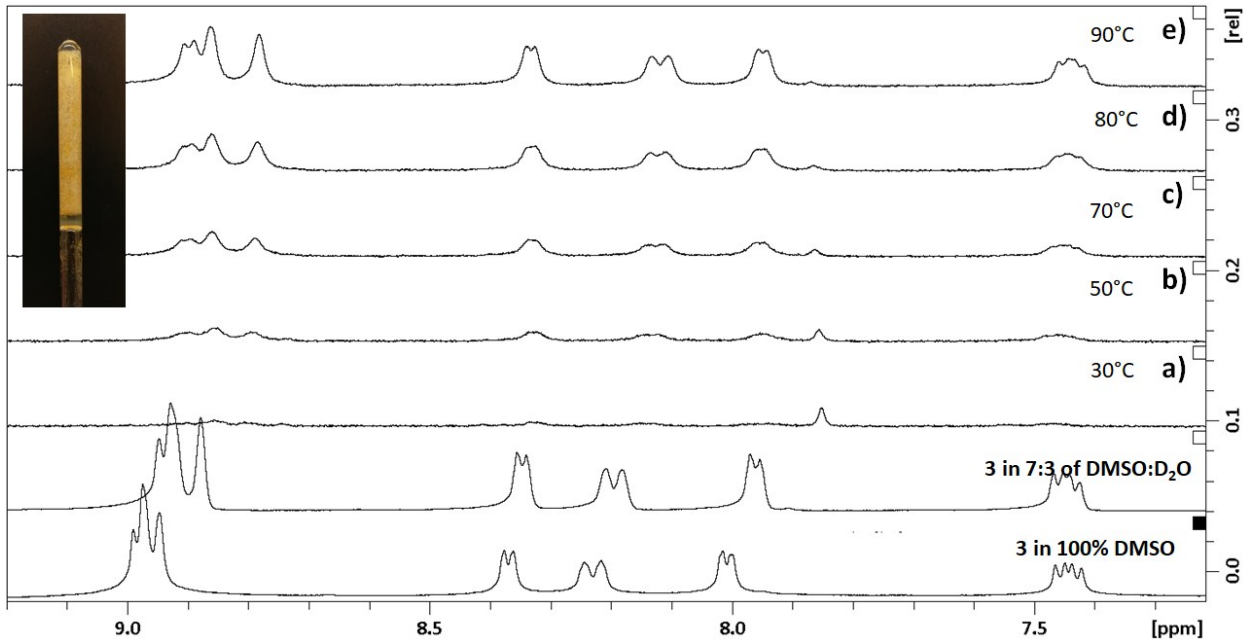

Figure S14. Temperature dependent ^{1}H-NMR spectra of [**3●AgNO$_3$**] gel system (1.6 x 10^{-2} M) from 7:3 of DMSO-d_6:D$_2$O (from 30 °C to 90 °C, 10 °C step increase). (Inlet figure: [**3●AgNO$_3$**] gel after VT NMR experiment)

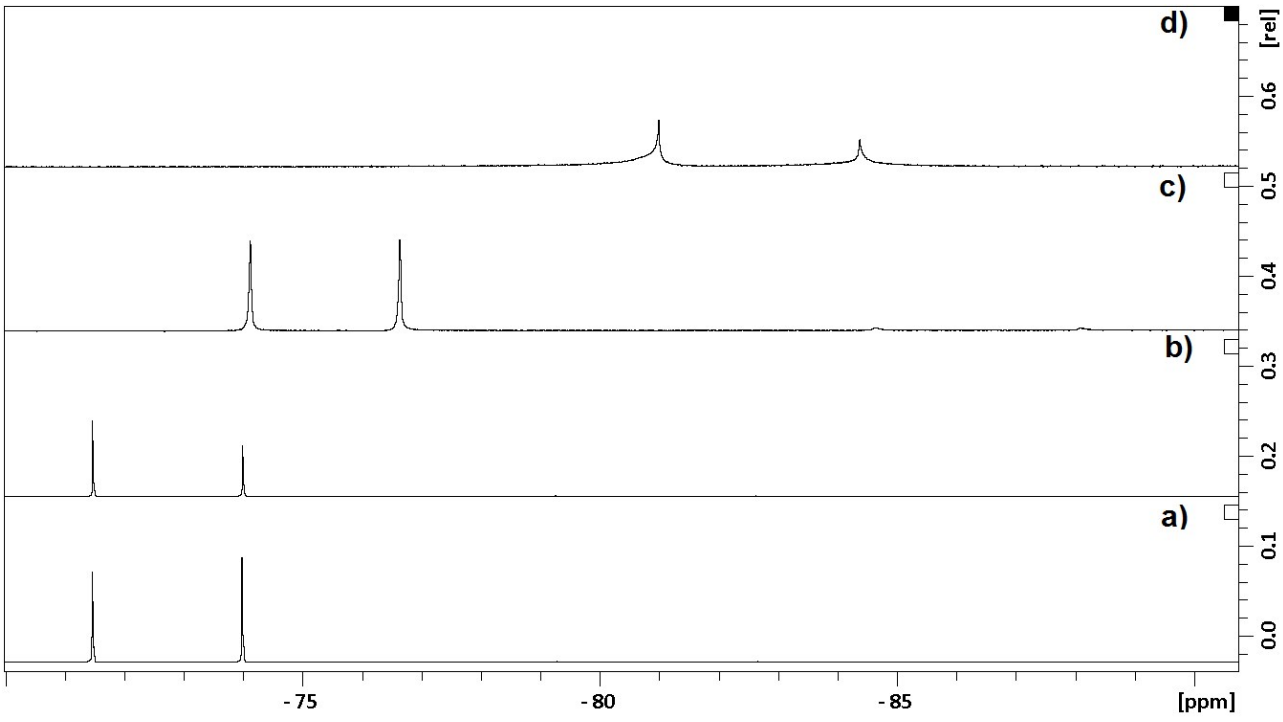

Figure S15. ^{19}F NMR: a) $AgPF_6$ b) 1_2+$AgPF_6$ (2.5 x 10^{-2} M) in pure DMSO-d_6 (δ= -71.46 and -73.98), c) 1_2+$AgPF_6$ gel from 3:7 of DMSO-d_6:D$_2$O (2.5 x 10^{-2} M; δ= -74.12 and -76.63), d) 3+$AgPF_6$ gel from 7:3 of DMSO-d_6:D$_2$O (1.6 x 10^{-2} M; δ= -81.00 and -84.38). External reference Aqueous F^- (KF), δ= -125.3

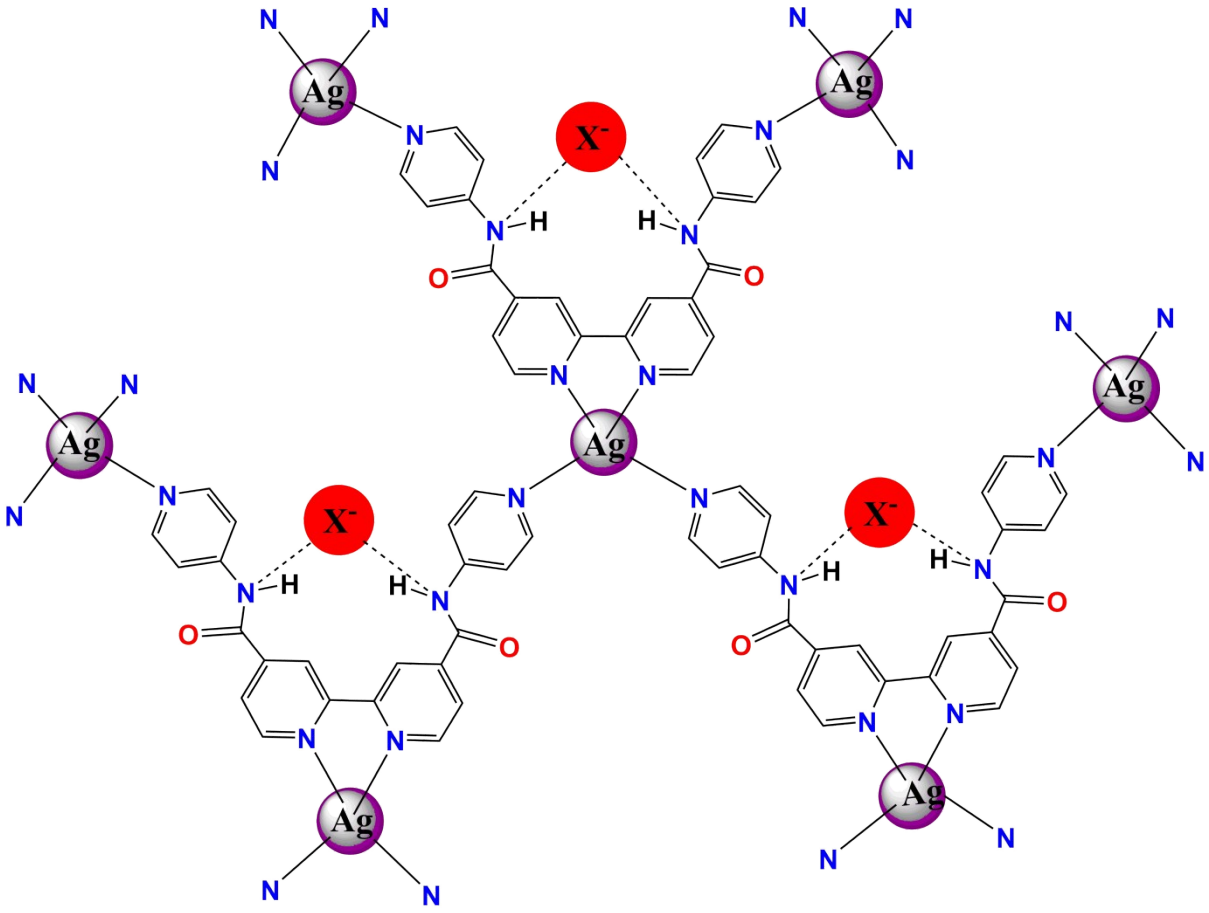

Figure S16. The proposed structure of the metallosupramolecular polymers **[4●AgX]$_n$** (X= NO_3^-, ClO_4^-, OTf^-, BF_4^- and PF_6^-).

X-ray crystallography

Single crystal X-ray structure determination: The single crystals of ligand (**4**) and Silver(I)-Coordination polymers of Ligands **1** were immersed in cryo-oil, mounted in a MiTeGen loop and measured at 120°C. The X-ray diffraction data were collected on an Agilent Technologies Supernova diffractometer using Mo Kα radiation. The *CrysAlisPro*[1] program packages were used for cell refinements and data reductions. Structures were solved by intrinsic phasing *SHELXT*[2] programs. Analytical or multi-scan absorption correction was applied to all data and structural refinements were carried out using *SHELXL*[2] and Olex2 graphical user interfaces[3] software. The hydrogen atoms were positioned geometrically and constrained to ride on their parent atoms, with C-H = 0.95-0.98 Å, N-H = 0.88 Å, and U_{iso} = 1.2-1.5·U_{eq} (parent atom). The crystallographic details are summarized in Table **S1** and **S2**.

Table S1. Crystallographic data for ligand **4**			
	4 in CH_3CN	**4 in DMF**	**4 in DMSO**
CCDC No	1823427	1823428	1823429
Formula	$C_{22}H_{16}N_6O_2$	$C_{22}H_{16}N_6O_2$, 2(C_3H_7NO)	$C_{22}H_{16}N_6O_2$, 2(C_2H_6OS)
Formula weight	396.41	542.60	552.66
Temp (K)	120	120	120
Crystal System	Monoclinic	Monoclinic	Triclinic
Space group	P21/c	C2/c	P-1
a (Å)	5.0978(5)	19.2704(6)	7.4404(5)
b (Å)	9.7374(8)	4.05485(13)	9.0236(7)
c (Å)	17.7601(17)	33.1511(1)	10.0764(7)
α (°)	90	90	89.276(6)
β (°)	92.193(9)	92.289(3)	72.988(6)
γ (°)	90	90	79.287(6)
V ($Å^3$)	880.95(14)	2588.30(14)	635.01(8)
d_{calc} (g/cm^3)	1.494	1.392	1.445
Z	2	4	1
μ (mm^{-1})	0.101	0.097	0.256
Ref.Collected	3521	16005	8538
Ind. Ref	1936	2634	2591
R_{int}	0.0261	0.0284	0.0222
F (000)	412.0	1144.0	290.0
GOF	1.109	1.070	1.047
R1[a] ($I \geq 2\sigma$)	0.0580	0.0459	0.0318
wR2b($I \geq 2\sigma$)	0.1288	0.1153	0.0771

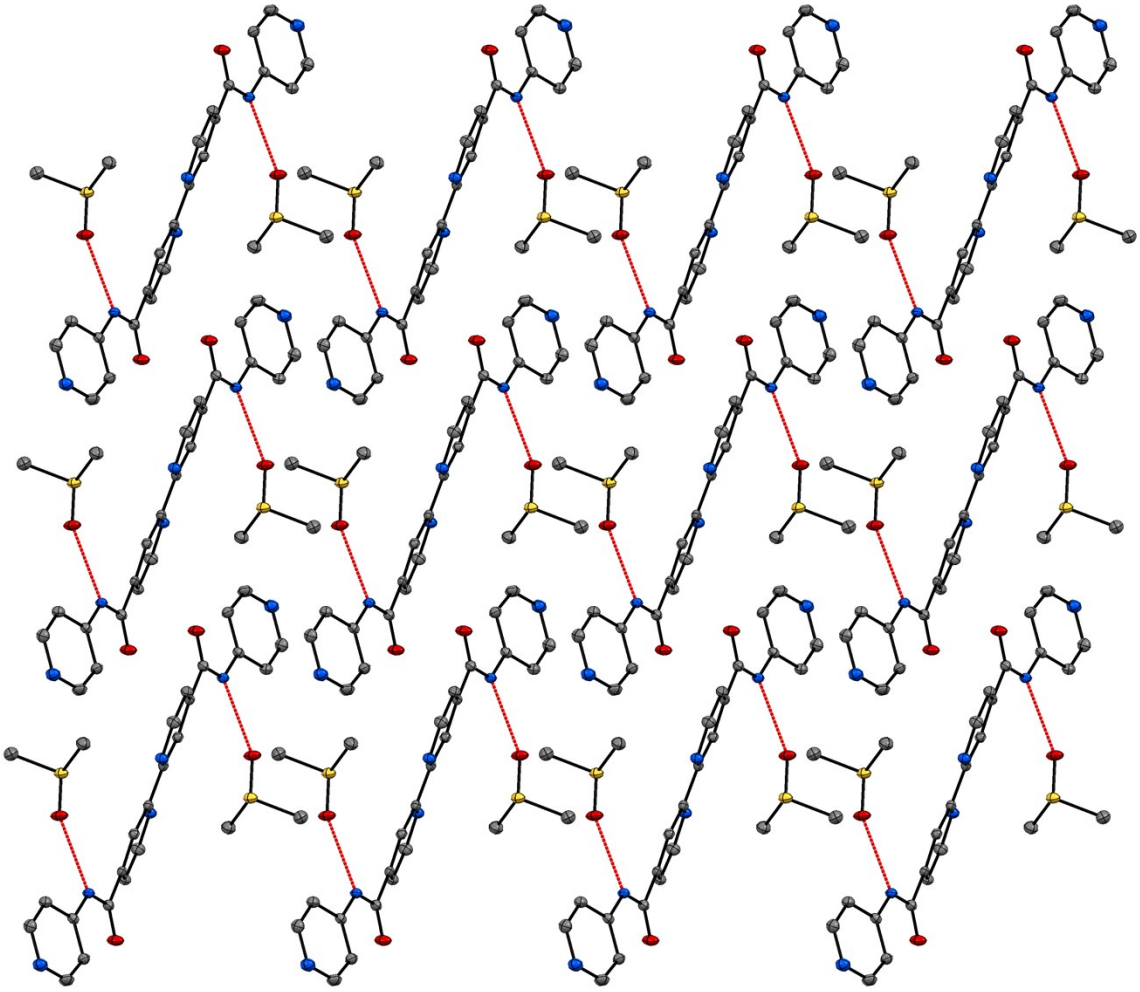

Figure S17. Crystal packing of ligand **4** in DMSO from a-axis.

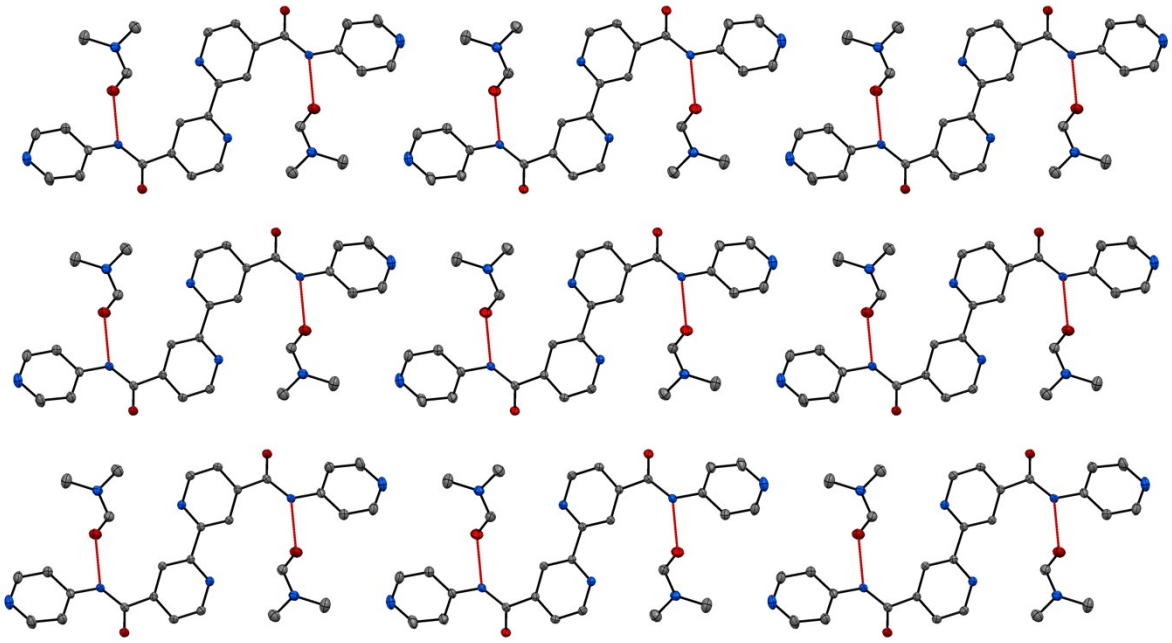

Figure S18. Crystal packing of ligand **4** in DMF from b-axis.

Table S2. Crystallographic data for CPs of **1** with different silver salts				
	[1_2●$AgClO_4$]	**[1_2●AgOTf]**	**[1_2●$AgPF_6$]**	**[1●AgOAc]**
CCDC No	1823430	1823431	1823432	1823433
Formula	$C_{22}H_{18}N_6O_2Ag$,	$C_{22}H_{18}N_6O_2Ag$,	$C_{22}H_{18}N_6O_2Ag$,	$C_{13}H_{12}N_3O_3Ag$
Formula weight	605.74	655.36	651.26	366.13
Temp (K)	120	120	120	120
Crystal System	Monoclinic	Monoclinic	Monoclinic	Triclinic
Space group	$P2_1/n$	$P2_1/n$	$P2_1/n$	P-1
a (Å)	11.3109(3)	11.84847(15)	11.5489(5)	7.3603(3)
b (Å)	14.7646(3)	11.65924(16)	11.6921(5)	8.6180(6)
c (Å)	13.9188(3)	18.1068(3)	18.1433(7)	11.0702(6)
α (°)	90	90	90	102.912(5)
β (°)	105.464(3)	101.3157(15)	101.463(4)	95.079(4)
γ (°)	90	90	90	108.486(5)
V (Å^3)	2240.30(9)	2452.73(6)	2401.04(2)	639.40(6)
d_{calc} (g/cm^3)	1.796	1.775	1.802	1.902
Z	4	4	4	2
μ (mm^{-1})	1.074	0.979	0.987	1.587
Ref.Collected	17283	19311	19526	9983
Ind. Ref	4585	5014	5273	3064
R_{int}	0.0266	0.0304	0.0472	0.0301
F (000)	1216.0	1312.0	1296.0	364.0
GOF	1.088	1.040	1.049	1.045
R1[a] ($I \geq 2\sigma$)	0.0269	0.0251	0.0319	0.0230
wR2b($I \geq 2\sigma$)	0.0580	0.0579	0.0772	0.0521

Table S3. Hydrogen-bond geometry (Å, °)					
	D–H···A	**D–H**	**H···A**	**D···A**	**D–H···A**
4 in CH_3CN	N2–H2···O1^{i}	0.88	2.18	2.972 (3)	149.6
4 in DMF	N2–H2···O2^{ii}	0.88	1.98	2.813 (2)	158.4
4 in DMSO	N2–H2···O2	0.88	2.01	2.849 (7)	158.3
[1_2●$AgClO_4$]	N2–H2···O6^{iii}	0.88	2.14	2.966 (2)	156.1
	N5–H5···O1^{iii}	0.88	2.47	2.984 (2)	117.9
	N5–H5···O3^{iV}	0.88	2.24	3.056 (3)	154.9
[1_2●AgOTf]	N2–H2···O3	0.88	2.18	3.005 (2)	154.8
	N5–H5···O4^{V}	0.88	2.39	3.180 (2)	149.4
[1_2●$AgPF_6$]	N2–H2···F1^{v}	0.88	2.31	3.126(2)	154.8
[1●AgOAc]	N2–H2···O2^{Vi}	0.88	1.92	2.760 (2)	158.6
Symmetry codes: (i) -1+X, +Y, +Z (ii) +X, -1+Y, +Z (iii) 1/2-X, -1/2+Y, 1/2-Z (iV) 3/2-X, -1/2+Y, 1/2-Z (V) 1-X, 1-Y, 1-Z (Vi) 1-X, 1-Y, 2-Z					

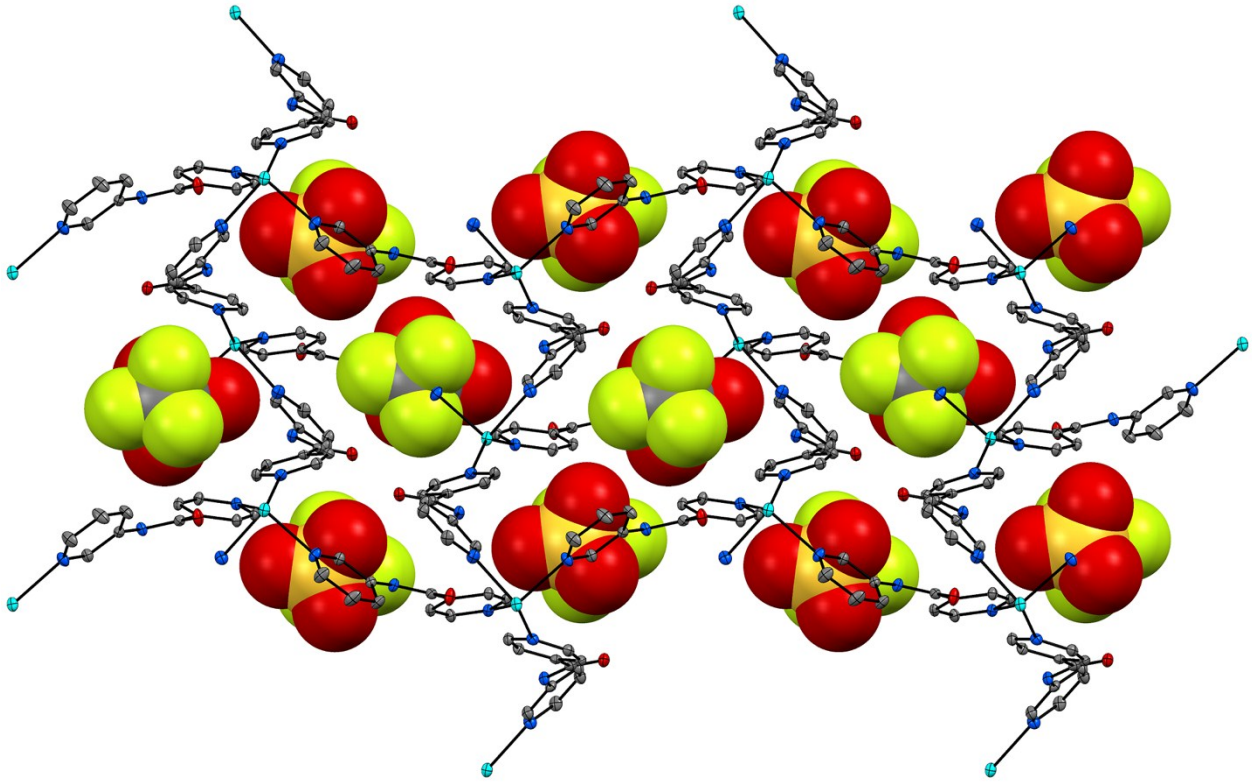

Figure S19. Crystal packing of **[1●AgOTf]** from a-axis.

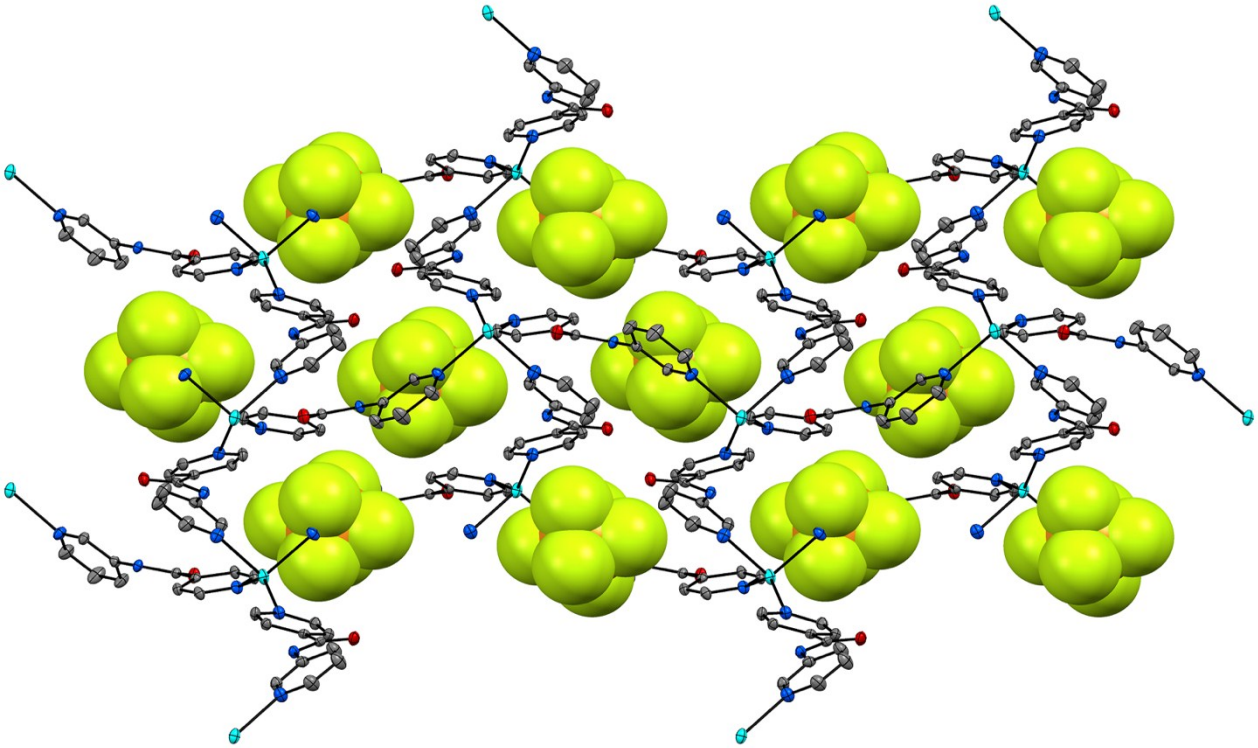

Figure S20. Crystal packing of [**1●AgPF$_6$**] from a-axis.

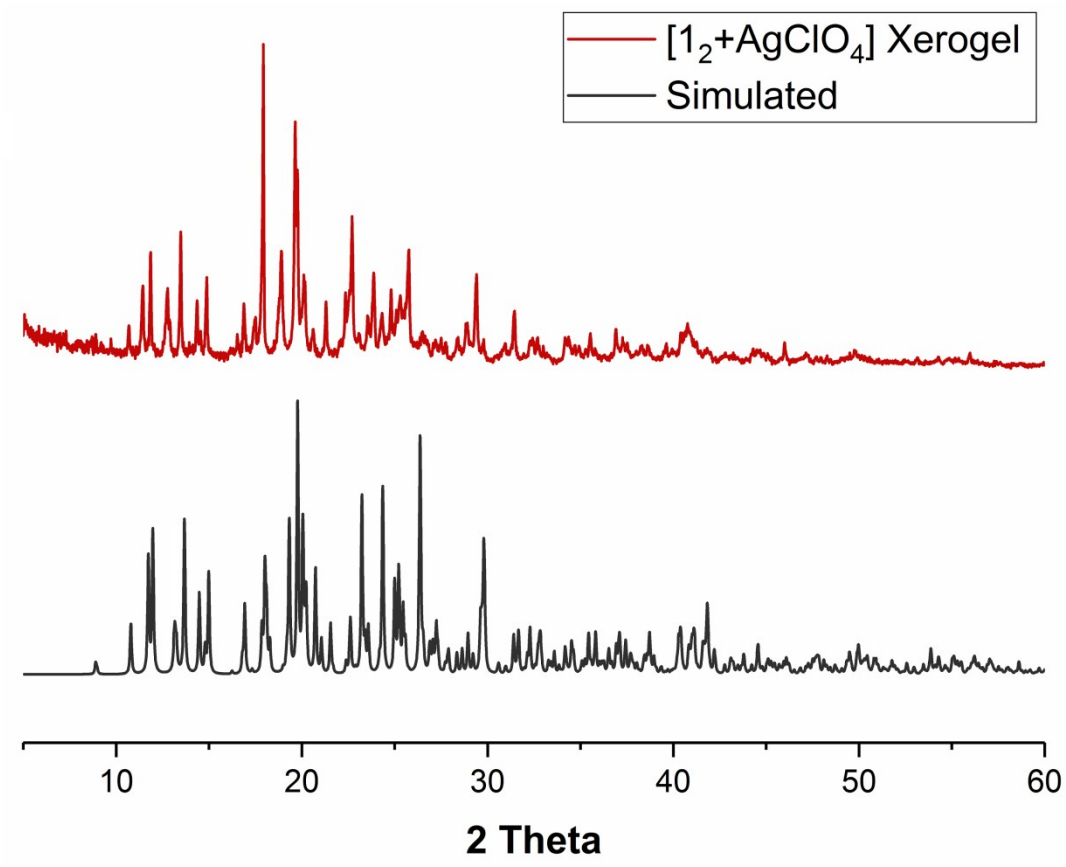

Figure S21 Comparison between the PXRD patterns of [**1$_2$+AgClO$_4$**]: simulated from single crystal X-ray structure (bottom) and xerogels sample (top).

Transmission electron microscopy (TEM)

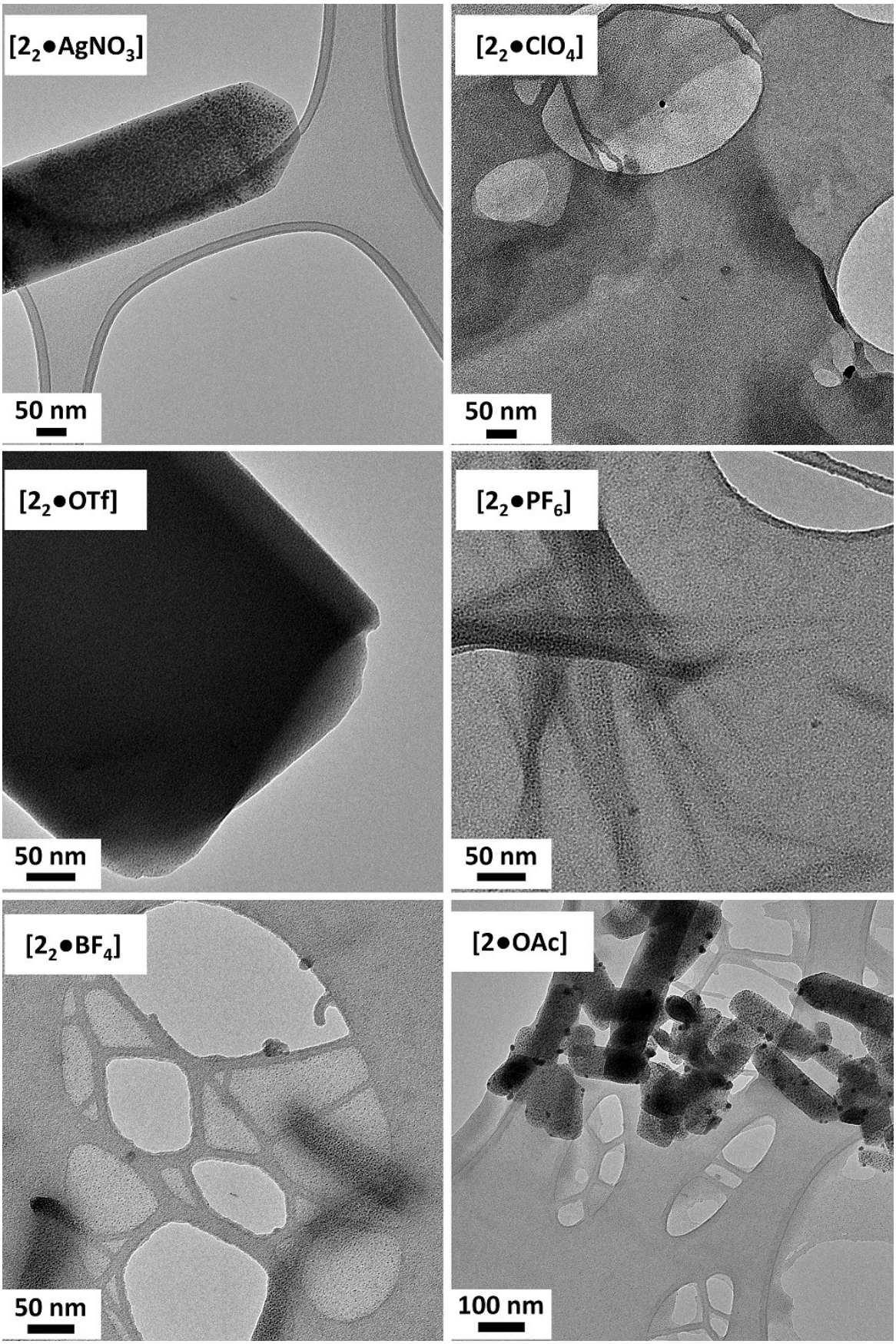

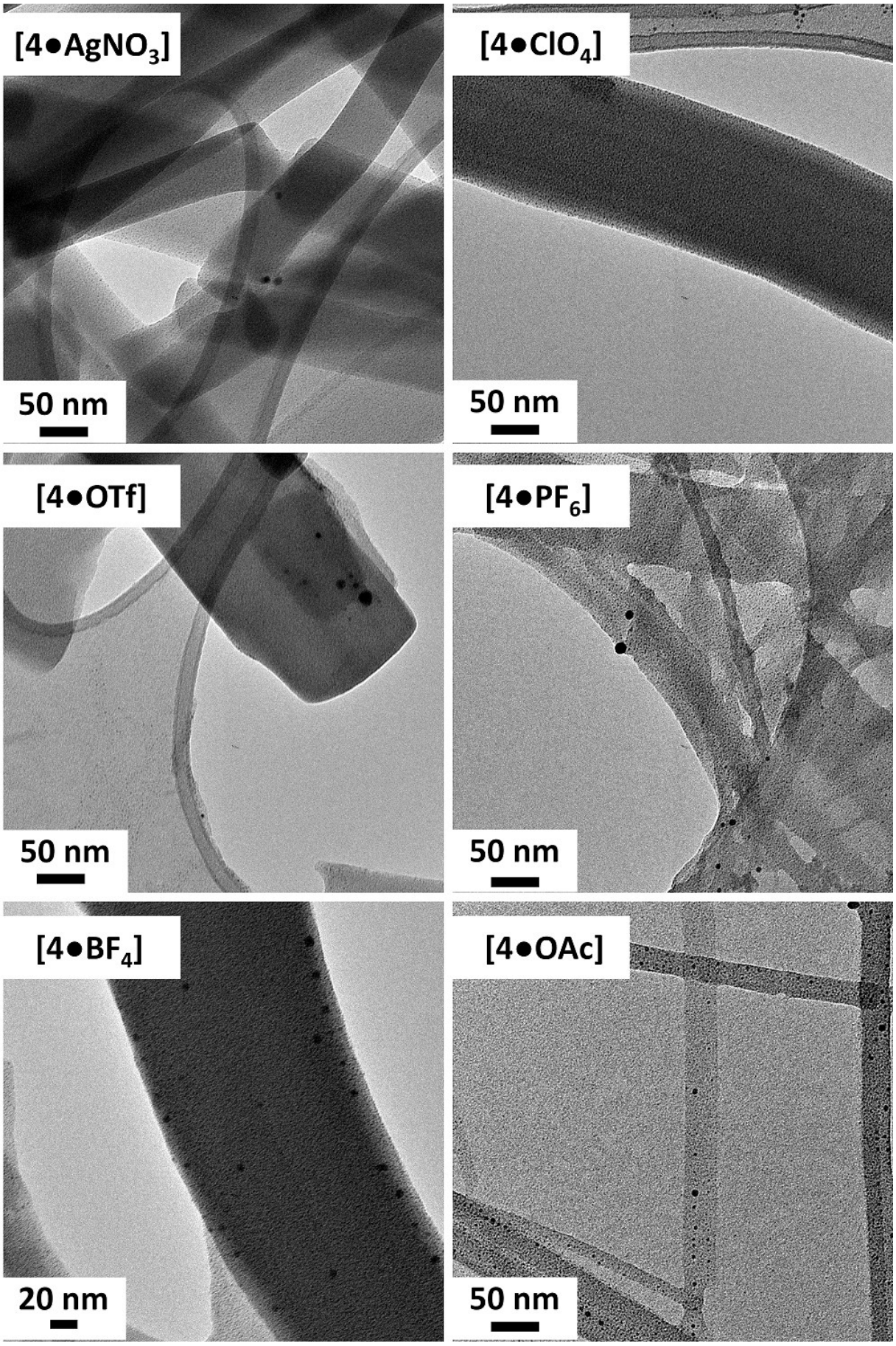
[4●AgNO3]
50 nm
[4●ClO4]
50 nm
[4●OTf]
50 nm
[4●PF6]
50 nm
[4●BF4]
20 nm
[4●OAc]
50 nm

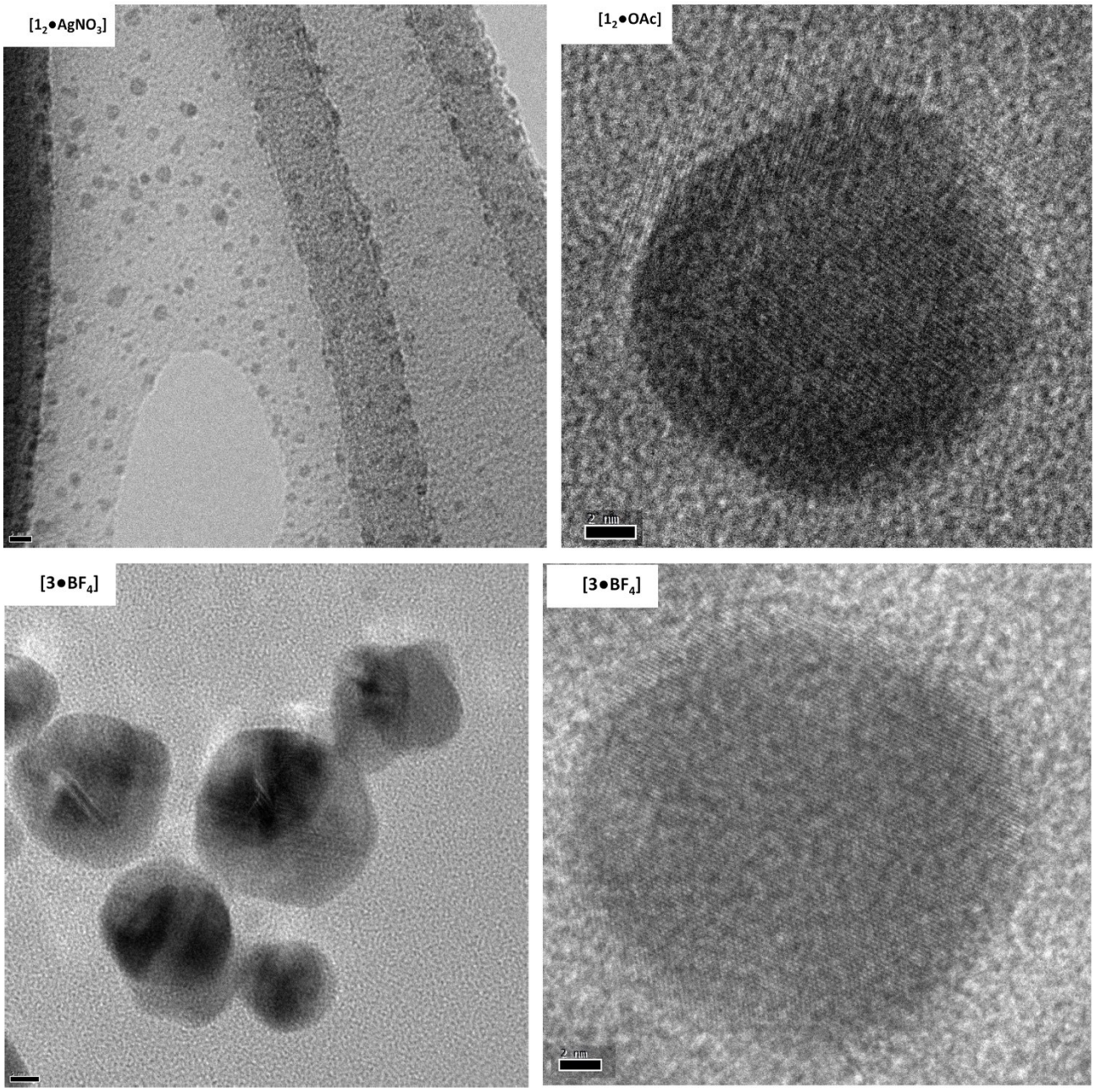
[1_2•$AgNO_3$]
[1_2•OAc]
2 nm
[3•BF_4]
[3•BF_4]
2 nm

Rheological Measurements

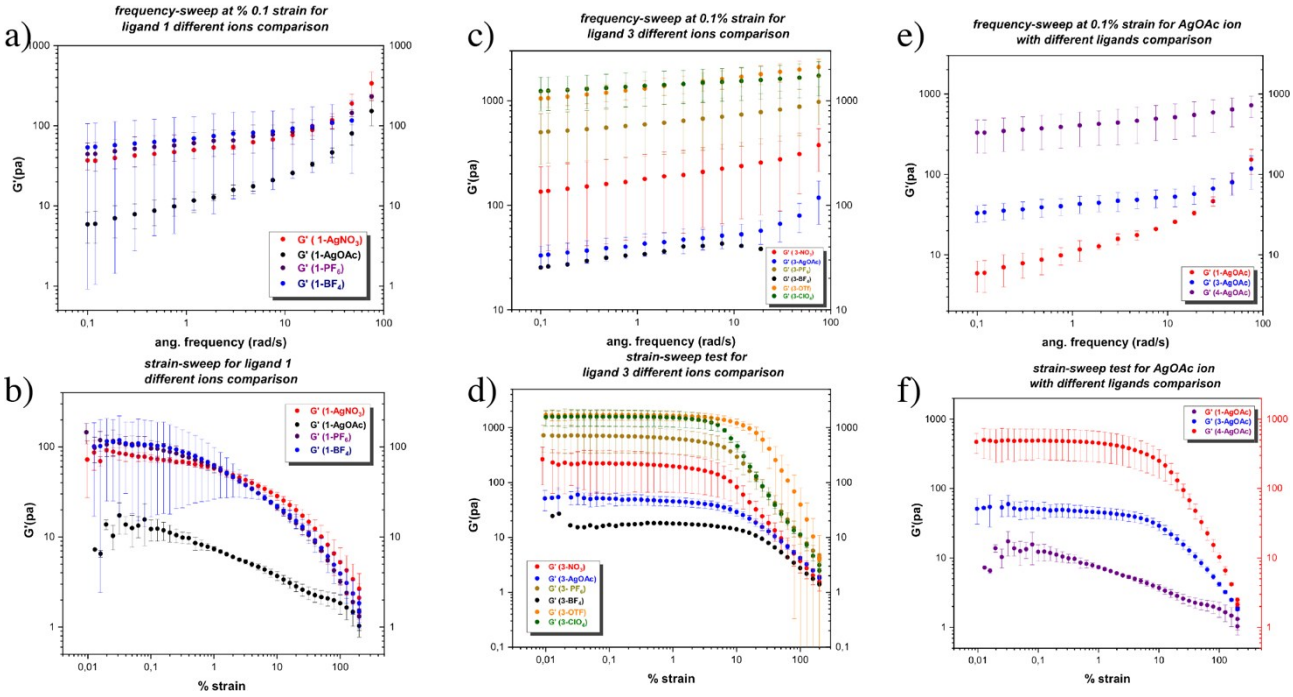

Figure S22. a,b) Frequency and strain sweep experiments performed for metallogels derived from ligand **1** with different silver salts and comparison of the gels strength. **c,d**) Frequency and strain sweep experiments performed for metallogels derived from ligand **3** with different silver salts and comparison of the gels strength. **e,f**) Frequency and strain sweep experiments performed for metallogels derived from ligand **1, 3 and 4** with AgOAc. Time sweep experiments were performed at frequency of 6.283 rad/s and 0.1% strain, frequency sweeps were collected at a strain value of 0.1% and strain sweeps were collected at frequency of 6.283 rad/s.

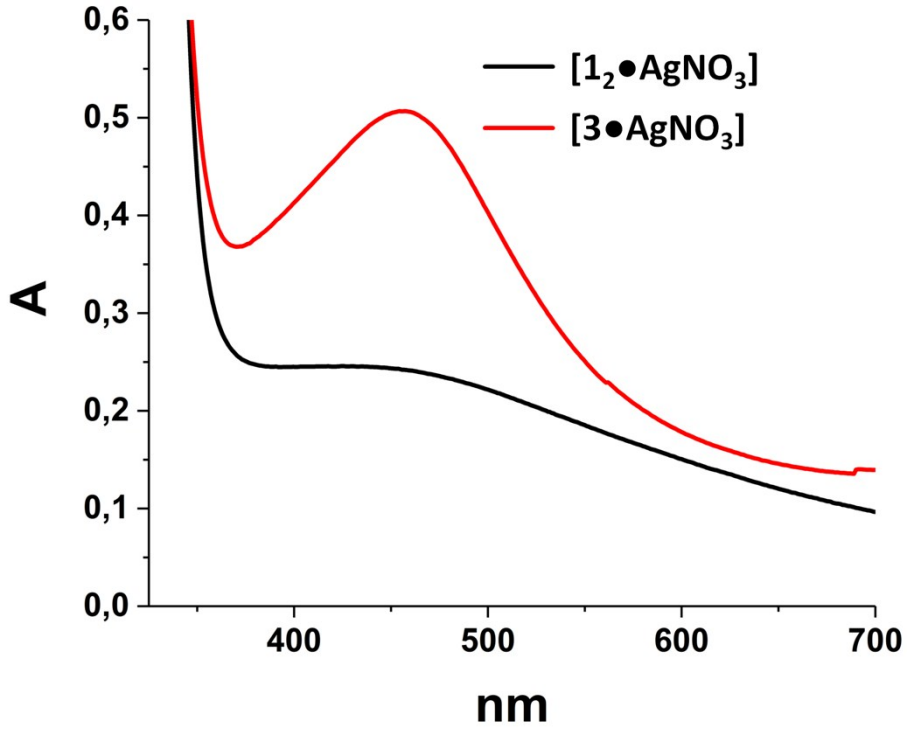

Figure S23 UV-vis spectra of metallogels prepared from **1** (5 x 10^{-3} M) and **3** (3.7 x10^{-3} M) in DMSO.

Photoluminescence

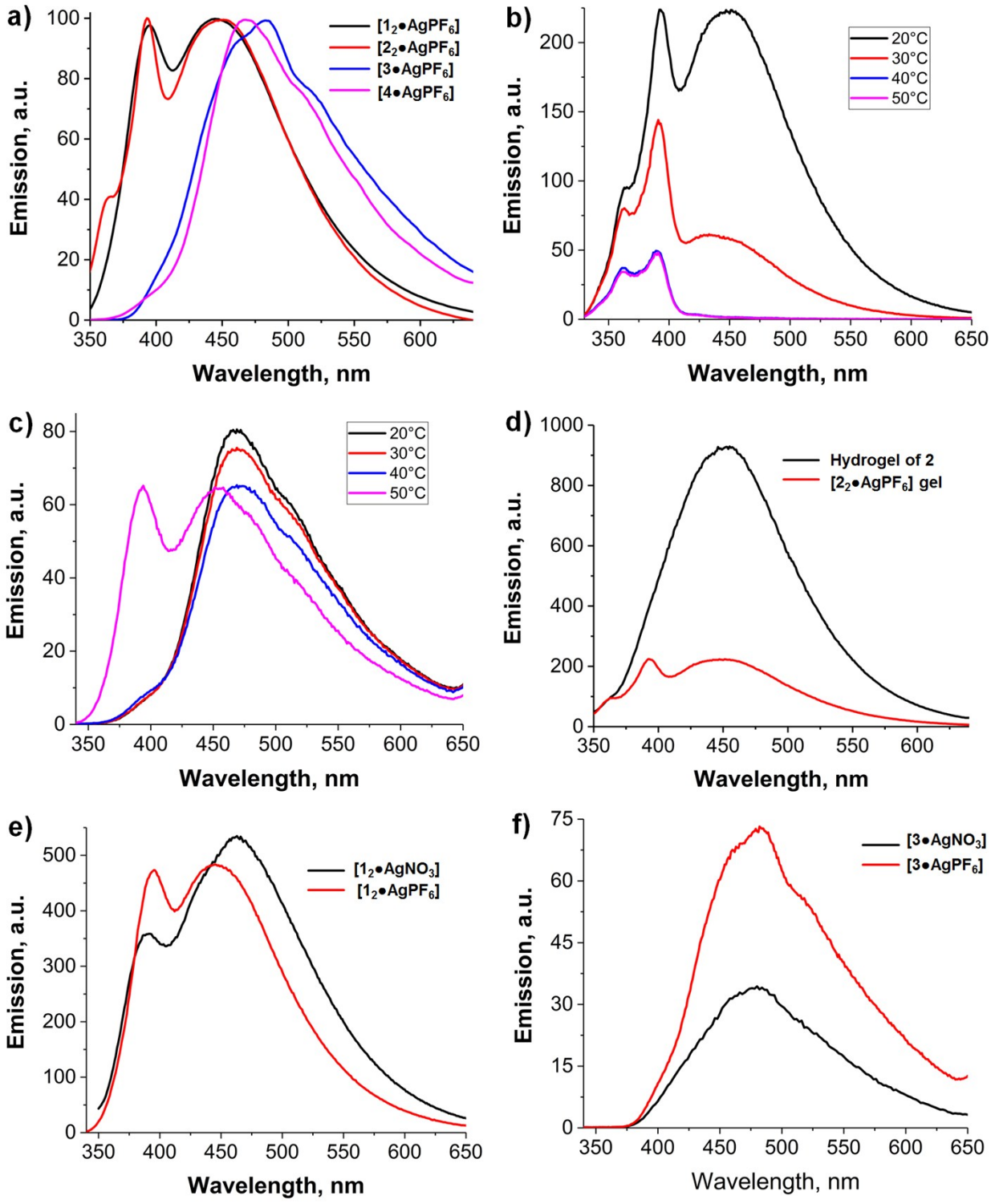

Figure S24. a) Normalized emission spectra of CPGs derived from ligands 1,2 (2 x 10^{-2} M) and 3,4 (1.5 x 10^{-2} M). b&c) Temperature-dependent emission spectra of **[2_2•AgPF$_6$]** (b) and **[3•AgPF$_6$]** (c) gels. d) Emission spectral comparison of Ligand **2** and **[2_2•AgPF$_6$]** gel. e&f). Emission spectral comparison of metallogels derived from ligands **1** and **3** with $AgNO_3$ and $AgPF_6$.

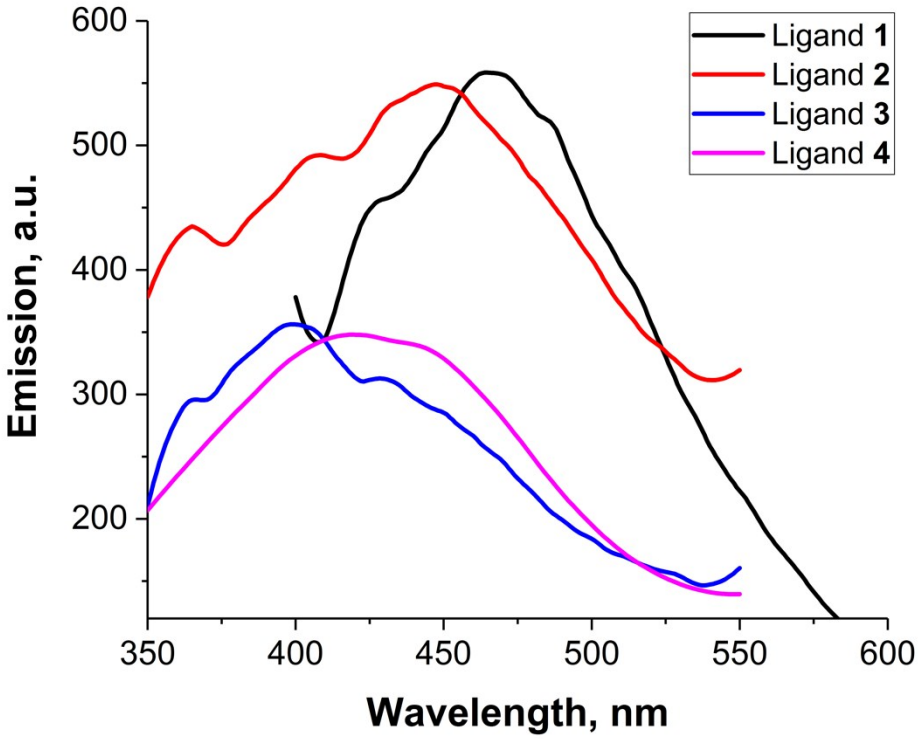

Figure S25. Emission spectra of solid ligands **1–4**.

References

1. Rigaku Oxford Diffraction, CrysAlisPro., **2013**, Yarnton, Oxfordshire, England.
2. G. M. Sheldrick, *Acta Cryst*., 2015, **C71**, 3–8; *Acta Cryst*., 2015, **A71**, 3–8.
3. O. V. Dolomanov, L. J. Bourhis, R. J. Gildea, A. J. K. Howard, and H. Puschmann, *J. Appl. Cryst*., 2009, **42**, 339–341.